Polymer Chemistry

Accepted Manuscript

ROYAL SOCIETY OF CHEMISTRY

www.rsc.org/polymers

Microporous spiro-centered poly(benzimidazole) networks: preparation, characterization, and gas sorption properties

Yan-Chao Zhao,[†,‡] Tao Wang,[†] Li-Min Zhang,[†] Yi Cui,[†,‡] Bao-Hang Han*[,†]

[†] *National Center for Nanoscience and Technology, Beijing 100190, China*

[‡] *Graduate University of Chinese Academy of Sciences, Beijing 100049, China*

Tel: +86 10 8254 5576. Email: hanbh@nanoctr.cn.

Table of Contents/Abstract Graphic

Microporous spiro-centered poly(benzimidazole) networks: preparation, characterization, and gas sorption properties

Yan-Chao Zhao,[†,‡] Tao Wang,[†] Li-Min Zhang,[†] Yi Cui,[†,‡] Bao-Hang Han*[,†]

Three microporous spiro-centered poly(benzimidazole) networks were synthesized based on the condensation of di-/trialdehyde with 3,3,3',3'-tetramethyl-1,1'-spirobisindane-5,5',6,6'-tatrone in refluxing glacial acetic acid containing ammonium acetate.

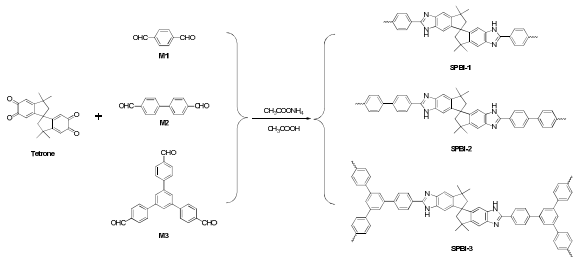

Abstract

Three microporous spiro-centered poly(benzimidazole) networks were synthesized based on the condensation of di-/trialdehyde with 3,3,3',3'-tetramethyl-1,1'-spirobisindane-5,5',6,6'-tatrone in refluxing glacial acetic acid containing ammonium acetate. Fourier transform infrared and solid-state cross-polarization/magic-angle-spinning ^{13}C NMR spectroscopy were utilized to confirm the presence of benzimidazole ring in the obtained polymers. The morphology can be observed from scanning electron microscopy and transmission electron microscopy images. The materials possess Brunauer–Emmet–Teller specific surface area ranging from 520 to 600 m^2 g^{-1}. The highest hydrogen and carbon dioxide sorption capacity of the obtained poly(benzimidazole) networks are up to 1.60 wt % (77 K and 1.0 bar) and 13.6 wt % (273 K and 1.0 bar), which are comparable with those of most of microporous organic polymers.

Keywords: microporous, spiro-centered, poly(benzimidazole), gas sorption

Introduction

During the past few years, microporous organic materials have attracted considerable attention due to their important applications as heterogeneous catalysts,[1] gas permeable membranes,[2] and gas storage materials.[3] They are totally composed of nonmetal elements, and possess large and accessible surface area and easily functionalized. Many classes of microporous organic materials have been prepared including hypercross-linked polymers, polymers of intrinsic microporosity, conjugated microporous polymers, and covalent organic frameworks. Generally, non-planar monomers and rigid linkages can create much free volume, i.e., microporosity.[4] Microporous poly(benzimidazole)s is an important type of conjugated micorporous polymers, since benzimidazole ring can add additional functions into polymer.

From the original zeolites and activated carbon to the advanced metal–organic frameworks,[5] covalent organic frameworks,[6] and polymeric networks,[7] the researches on microporous materials have been lasted for decades. Microporous organic polymers (MOPs), containing hypercross-linked polymers,[8] conjugated microporous polymers,[9] polymeric organic frameworks,[10] and polymers of intrinsic microporosity (PIMs)[11] have drawn a large amount of attention owing to their important applications. The appearance of PIMs sheds a light on the development of the MOPs since it was first reported in 2002.[12] PIMs are rigid and contorted networks, which wholly consist of fused-ring formation, which could not be packed so efficiently as to leave much free volume, i.e., microporosity.[13]

For PIMs, rigid and spiro-structured monomers are necessary. Spiro(fluorine-9,9′-xanthene), with the fluorine and xanthene moieties connected by a tetrasubstituted carbon atom spiro-center, was used to prepare porous organic polymers through Sonogashira–Hagihara and Suzuki coupling reactions.[14] Given the request on the structure of monomers, another interesting molecule comes in sight. Triptycene, with three-dimensional spatial orientation, contains three benzene rings in a paddle-wheel configuration. The unusual conformation makes it derive a rigid monomer to prepare microporous materials. McKeown and his coworkers have taken advantages of the triptycene to synthesize a series of PIMs of which the Brunauer–Emmet–Teller specific surface area can be tuned between 618 and 1760 $m^2 g^{-1}$ by means of changing alkyl groups attached to their bridgehead positions.[3] As a famous microporous material, PIM-1 came into existence via the dioxane-forming reaction between 5,5',6,6'-tetrahydroxy-3,3,3',3'-tetramethyl-1,1'-spirobisindane and 2,3,5,6-tetrafluoroterephthalonitrile.[15] The representative soluble polymer, as a result of the site of contortion, can be made into another attractive polymer with characteristic and outstanding carbon dioxide separation performance by the cycloaddition reaction between aromatic nitrile groups and sodium azide.[2] Polyimides are usually made from a diamine and a bis(carboxylicanydride) by means of the cycloimidization reaction. Using the 5,5',6,6'-tetrahydroxy-3,3,3',3'-tetramethyl-1,1'-spirobisindane as a precursor, a kind of solution-processable membrane that has a high permeability for carbon dioxide was prepared.[16]

Porous poly(benzimidazole) (PBI) networks were once prepared by Weber et al. though a hard-templating process but what was a pity that the specific surface area values were relatively low from 100 to 200 m^2 g^{-1}.[17] After that, El-Kaderi et al. motivated the preparation of PBI networks through the condensation between *o*-phenylenediamine and aldehyde without any templates.[18] Despite all of the approaches for synthesis of PBI networks, we also took account of such a classic route that diketone could react with aldehyde monomers in refluxing glacial acetic acid containing ammonium acetate to form a imidazole ring.[19] The adsorption quantity of gas (i.e., hydrogen and carbon dioxide) of PBI networks could be heightened as a result of the fact that hetero nitrogen atoms in the skeleton of PBI networks may enhance the dipole–dipole interactions between the adsorbate and the adsorbent.[20] Considering the aim of the porous materials, we construct the PBI networks by the condensation of 3,3,3',3'-tetramethyl-1,1'-spirobisindane-5,5',6,6'-tetrone and aromatic aldehyde to make a series of MOPs named as spiro-centered poly(benzimidazole) (**SPBI**) networks. This condensation was used to synthesize PBI networks with no templates, catalysts, or byproducts. With high specific surface area values over 600 m^2 g^{-1}, the gas storage (hydrogen and carbon dioxide) capacities were investigated.

Experimental

Materials and methods

Glacial acetic acid, ammonium acetate, concentrated nitric acid, and terephthalic

aldehyde were purchased from Beijing chemical reagent company, and terephthalic aldehyde was purified by recrystallization in ethanol. 4-Formylphenylboronic acid, 1,3,5-tribromobenzene, 5,5',6,6'-tetrahydroxy-3,3,3',3'-tetramethyl-1,1'-spirobisindane, and bis(triphenylphosphine)palladium(II) dichloride were purchased from Aldrich. 4,4'-Biphenyldicarboxaldehyde, 1,3,5-tris(4-formylphenyl)benzene, and 3,3,3',3'-tetramethyl-1,1'-spirobisindane-5,5',6,6'-tetrone were synthesized according to the reported procedures, respectively. [21] ,[15] Ethyl acetate, petroleum ether, dichloromethane, acetone, and other chemical reagents were used as received. All condensation reactions were operated using standard Schlenk line technique.

Preparation of spiro-centered microporous poly(benzimidazole) networks (SPBI)

A mixture of terephthalic aldehyde (12 mg, 0.09 mmol), 3,3,3',3'-tetramethyl-1,1'-spirobisindane-5,5',6,6'-tatrone (30 mg, 0.09 mmol), and ammonium acetate (208 mg) was suspended in glacial acetic acid (4.00 mL). After ultrasonicaion for 0.5 h, the mixture was degassed by at least three freeze–pump–thaw cycles. After 180 °C for 72 h, the reaction mixture gave a yellow solid in 83 % yield. This solid, denoted **SPBI-1**, was filtrated and washed with acetone, dichloromethane, and ethanol subsequently. The product was dried *in vacuo* at 120 °C for more than 12 h.

Similar to the preparation of **SPBI-1**, 4,4'-biphenyldicarboxaldehyde (19 mg, 0.09 mmol) and 1,3,5-tris(4-formylphenyl)benzene (23 mg, 0.06 mmol) were used to afford **SPBI-2** and **SPBI-3** in 70–80 % yields, respectively.

Instrumental characterization

^{1}H NMR spectra were recorded on a Bruker DMX400 NMR spectrometer, with tetramethylsilane as an internal reference. Solid-state ^{13}C CP/MAS NMR measurements were performed on a Bruker Avance III 400 spectrometer. Thermogravimetric analysis (TGA) was performed on a Pyris Diamond thermogravimetric/differential thermal analyzer by heating the samples at 10 °C min^{-1} to 800 °C in the atmosphere of nitrogen. Infrared (IR) spectra were recorded in KBr pellets using a Spectrum One Fourier transform infrared (FT-IR) spectrometer (PerkinElmer Instruments Co. Ltd, USA). The sample was prepared by dispersing the polymers in KBr and compressing the mixtures to form disks, and 15 scans were signal-averaged. Transmission electron microscopy (TEM) observations were carried out using a Tecnai G^{2} F20 U-TWIN microscope (FEI, USA) at an accelerating voltage of 200 kV. Energy dispersive X-ray (EDX) detector was used to analyze the chemical elements of the samples. The sample was prepared by dropping an ethanol suspension of **SPBI-1**–**SPBI-3** onto a copper grid, respectively. Field emission scanning electron microscopy (SEM) observations were performed on a Hitachi S-4800 microscope (Hitachi, Ltd. Japan) operating at an accelerating voltage of 6.0 kV. SEM samples were prepared by dropping an ethanol suspension of **SPBI-1**–**SPBI-3** on a silicon wafer and left to dry in air. Nitrogen adsorption−desorption and hydrogen adsorption experimentations were conducted using an ASAP 2020 M+C accelerated surface area and porosity analyzer (Micromeritics,

USA). Carbon dioxide uptake experimentation was performed by using a TriStar II 3020 surface area and porosity analyzer (Micromeritics, USA). Before measurement, the samples were degassed *in vacuo* at 120 ℃ for more than 12 h. Specific surface area was calculated from nitrogen adsorption data by Brunauer–Emmett–Teller (BET) analysis, while pore size and pore size distribution were estimated through the original density function theory (DFT). Total pore volume was calculated from nitrogen adsorption–desorption isotherms at $P/P_0 = 0.99$.

Results and discussion

4,4'-Biphenyldicarboxaldehyde and 1,3,5-tris(4-formylphenyl)benzene was synthesized by Suzuki coupling reaction of 4-formylphenylboronic acid with 4-bromobenzaldehyde and 1,3,5-tribromobenzene, whereas terephthalic aldehyde can be purchased from chemical reagent company. Oxidation of the 5,5',6,6'-tetrahydroxy-3,3,3',3'-tetramethyl-1,1'-spirobisindane with nitric acid produces 3,3,3',3'-tetramethyl-1,1'-spirobisindane-5,5',6,6'-tatrone, which reacts with di-/trialdehyde in refluxing glacial acetic acid containing ammonium acetate in good yields (70–80 %) to provide microporous spiro-centered poly(benzimidazole) networks (Scheme 1). The reactants and solvent were heated at 180 °C for 72 h in a sealed tube to form spiro-centered microporous poly(benzimidazole) networks. This condensation reaction is similar to our previously reported method.[22] All of the obtained polymers are stable and insoluble in common organic solvents, such as acetone, dichloromethane,

ethanol, and *N*,*N*-dimethylformamide.

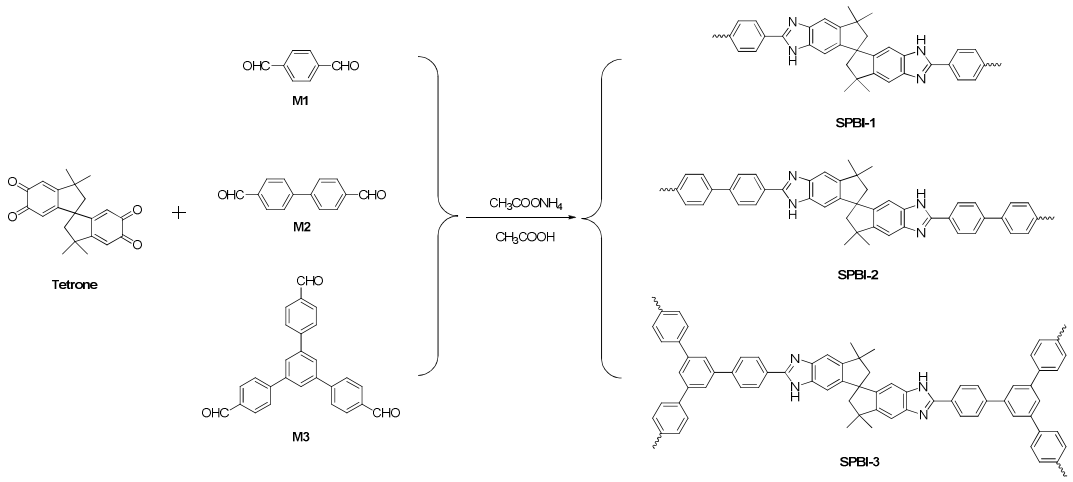

Scheme 1. Schematic representation of the preparation of microporous spiro-centered poly(benzimidazole) networks (**SPBI-1–SPBI-3**)

The spiro-centered benzimidazole linked polymers were confirmed by Fourier transform infrared (FT-IR) spectroscopy. In the spectra of the three polymers, bands which can be attributed to the carbonyl stretching of tetrone and dialdehyde monomers at 1660–1670 cm^{-1} are absent (Figs. 1 and S1–S2, see ESI). The stretching vibration of –*C*(=O)–*H* at 2870 cm^{-1} also disappears. Absorption peaks at 1600 cm^{-1} assigned to the stretching vibration of carbon–nitrogen double bond (–*C*=*N*–) indicate the occurrence of condensation. The characteristic aromatic and aliphatic C–H stretching vibration bands at ca. 3100 and 2990 cm^{-1} are also observed, which are derived from 3,3,3',3'-tetramethyl-1,1'-spirobisindane building blocks. Significantly, the three polymers exhibit a diagnostic band at 1450 cm^{-1} for the skeleton stretching vibration of

benzimidazole ring,[23] which is similar to the results of the FI-IR spectra of triptycene-based microporous poly(benzimidazole) networks.[22]

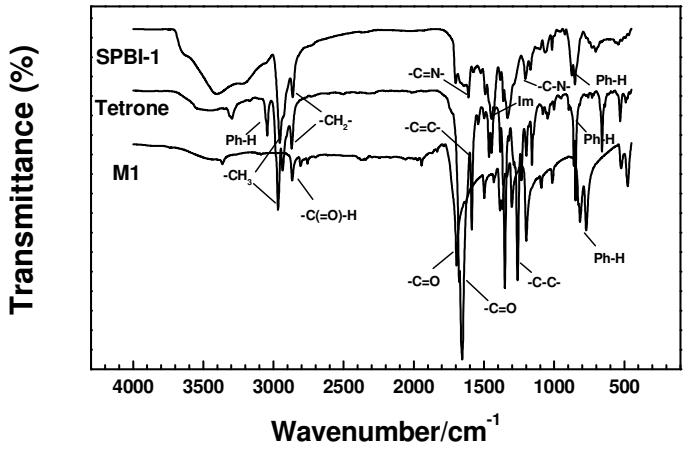

Fig. 1. FT-IR spectra of terephthalic aldehyde, tetrone monomer, and **SPBI-1**.

A more detailed analysis of the structure of the obtained polymers was performed by solid-state ^{13}C CP/MAS NMR spectroscopy, as shown in the Figs. 2 and S3–S4 (see ESI). The resonances at 58, 44, and 31 ppm can be unambiguously assigned to the quaternary carbon atom, methylene carbon atom, and methyl carbon atom, respectively, indicating the successful incorporation of the methyl-1,1'-spirobisindane unit into the networks. The seven signals between 156 and 105 ppm can be ascribed to the carbon atoms of aromatic rings. Most importantly, the peak at 161 ppm is observed in the obtained polymers, which corresponds to the carbon atom of benzimidazole, indicative of the successful build-up of benzimidazole-linked polymeric network. These results are also similar to our previously reported paper.[22]

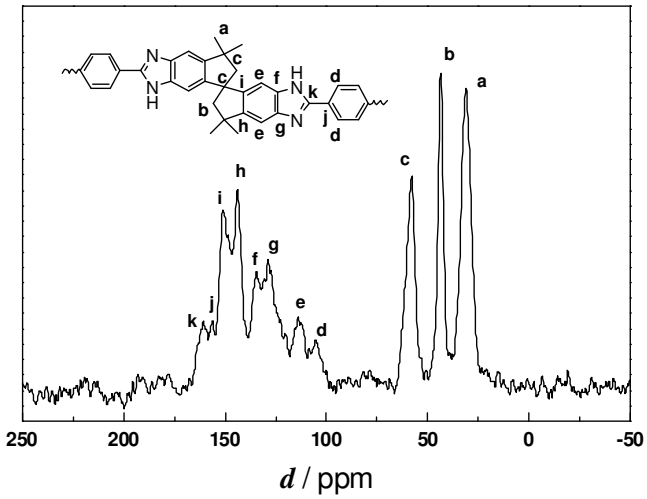

Fig. 2. Solid-state ^{13}C CP/MAS spectrum of **SPBI-1** recorded at the MAS rate of 5 Hz.

The morphology of the obtained polymers was investigated using scanning electron microscopy (SEM) measurements, while the local structure was observed through transmission electron microscopy (TEM). Seen from the SEM images, these polymers consist of a series of various agglomerated, interconnected, and regular-shaped microparticles. (Figs. 3 and S5, see ESI) The TEM images confirm that they possess a disorder and amorphous structure. These observations are consistent with other amorphous microporous organic polymers.[24]

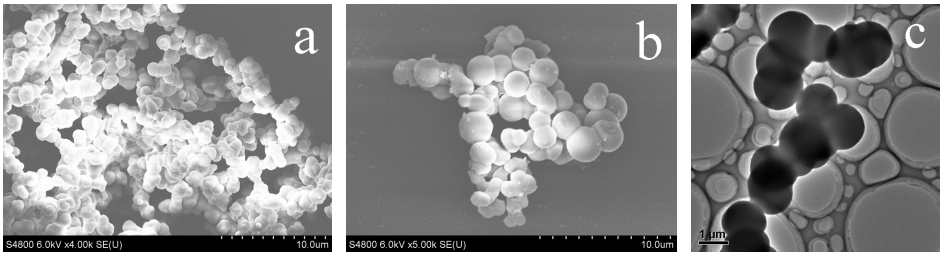

Fig. 3. SEM (a and b) and TEM (c) images of **SPBI-1** (a), **SPBI-2** (b), and **SPBI-3** (c).

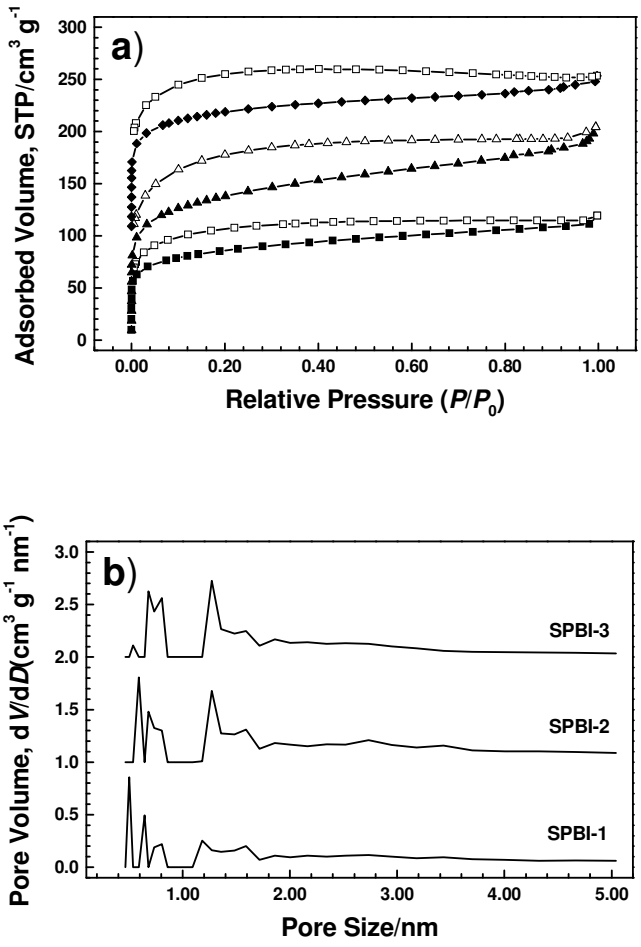

Fig. 4. (a) Nitrogen adsorption–desorption isotherms of **SPBI-1** (square), **SPBI-2** (uptriangle), and **SPBI-3** (diamond) at 77 K. The isotherm of **SPBI-2** and **SPBI-3** has been offset by 50 cm^3 g^{-1} for the purpose of clarity. (b) Pore size distribution profiles calculated by the original DFT method. The profiles of **SPBI-2** and **SPBI-3** have also been offset by 1 unit for the purpose of clarity.

The porosity of the obtained polymers was investigated by nitrogen sorption experiments at 77 K. Fig. 4a shows the nitrogen adsorption–desorption isotherms of **SPBI-1**, **SPBI-2**, and **SPBI-3**. The isotherms show a steep gas uptake at the relative pressure (P/P_0) less than 0.10, a relative flat uptake in the intermediate section, and a

weak hysteresis between adsorption and desorption branches, indicating a dominated microporosity and some little meso-/macroporosity in the obtained polymeric materials. However, the sorption hysteresis at the middle relative pressure can be interpreted as the network smelling or restricted access of nitrogen molecule to narrow pore opening,[25] especially for soft polymers. The specific surface area data of SPBIs calculated using Brunauer–Emmet–Teller (BET) model are 600, 520, and 590 $m^2 g^{-1}$, respectively.

The pore size distribution (PSD) profiles calculated from original density functional theory (DFT) using adsorption branch were shown in the Fig. 4b. There are several sharp peaks in the micropore area, which are centered at ca 0.70 and 1.20 nm. Additionally, one dominate peak located at 0.50–0.60 nm is also observed in the PSD profiles of **SPBI-1** and **SPBI-2**.

The narrow peaks less than 1.0 nm in Fig. 4b might be responsible for the gas sorption towards energy-related small molecules such as hydrogen and carbon dioxide.[26] Therefore, the **SPBIs** were subjected to carry out the hydrogen uptake and carbon dioxide capture experiments by volumetric methods. Fig. 5 shows their gravimetric adsorption isotherms. Hydrogen uptake capacities for these polymers are up to 1.60, 1.31, and 1.48 wt % at 77 K and 1.0 bar, whereas carbon dioxide capture capacities are up to 13.6, 8.4, and 11.7 wt % at 273 K and 1.0 bar. These values are reasonable for microporous organic polymers, whose specific surface area values are less than 600 $m^2 g^{-1}$.[27] In general, the higher BET specific surface area, the higher gas uptake capacity. This high gas (hydrogen and carbon dioxide) uptake capacity might be

attributed to the high affinity towards carbon dioxide through a strong dipole−dipole interaction and acid−base interaction by protonated and deprotonated of the imidazole ring.

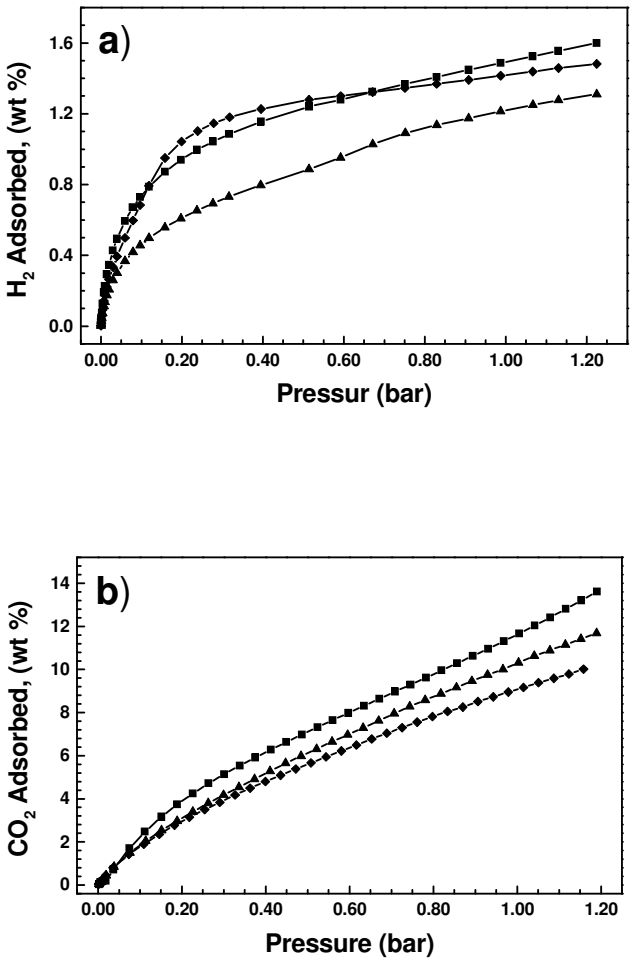

Fig. 5. Gravimetric hydrogen (a) and carbon dioxide (b) adsorption isotherms for **SPBI-1** (square), **SPBI-2** (uptriangle), and **SPBI-3** (diamond) at 77 K and 273K, respectively.

Conclusion

We have demonstrated a one-pot approach to prepare microporous spiro-centered poly(benzimidazole) networks through condensation of 3,3,3',3'-tetramethyl-1,1'-spirobisindane-5,5',6,6'-tatrone with di-/trialdehyde in refluxing glacial acetic acid containing ammonium acetate. This classic condensation is a catalyst-free and template-free process. The FT-IR and solid-state 13C NMR spectroscopy support the proposed structures in the obtained polymers. The highest BET specific surface area among these kinds of microporous materials is as high as 600 $m^2 g^{-1}$. Additionally, the materials possess nice hydrogen storage (1.60 wt %, 77 K and 1.0 bar) and carbon dioxide uptake (13.6 wt %, 77 K and 1.0 bar) properties. Overall, we extended the construction of microporous triptycene-based poly(benzimidazole) networks into microporous spiro-centered poly(benzimidazole) networks and explored further applications.

Acknowledgements

The financial support of the National Natural Science Foundation of China (Grant no. 21374024 and 61261130092), the Ministry of Science and Technology of China (Grant no. 2014CB932200) is acknowledged.

Electronic supplementary information (ESI) available: Details of synthetic procedures of monomers and FT-IR data.

References

(1) H. J. Mackintosh, P. M. Budd and N. B. Mckeown, Catalysis by microporous phthalocyanine and porphyrin network polymers. *J. Mater. Chem.*, 2008, **18** (5), 573–578.

(2) N.-Y. Du, H. B. Park, G. P. Robertson, T. Visser, L. Scoles and M. D. Guiver, Polymer nanosieve membranes for CO_2-capture applications. *Nat. Mater.*, 2011, **10** (5), 372–375.

(3) B. S. Ghanem, M. Hashem, K. D. Marris, K. J. Msayib, M.-C. Xu, P. M. Budd and N. B. Mckeown, Triptycene-based polymers of intrinsic microporosity: organic materials that can be tailored for gas adsorption. *Macromolecules*, 2010, **43** (12), 5287–5294.

(4) N. B. Mckeown, P. M. Budd and D. Book, Microporous polymers as potential hydrogen storge materials. *Macromol. Rapid Commun.*, 2007, **28** (9), 995–1002.

(5) M. Eddaoudi, J. Kim, N. Rosi, D. Vodak, J. Wachter and O. M. Yaghi, Systematic design of pore size and functionality in isoreticular MOFs and their applications in methane storge. *Science*, 2002, **295**, 469–453.

(6) J. M. Colson, A. R. Woll, A. Mukherjee, M. P. Levendorf, E. L. Spitler and W. R. Dichtel, Oriented 2D covalent organic framework thin films on single-layer graphene. *Science*, 2011, **332**, 228–232.

(7) Y.-C. Zhao, D. Zhou, Q. Chen, X.-J. Zhang, N. Bian, A.-D. Qi and B.-H. Han, Thionyl chloride-catalyzed preparation of microporous organic polymers through aldol condensation. *Macromolecules*, 2011, **44** (16), 6382–6388.

(8) M. P. Tsyurupa and V. A. Davankov, Hypercrosslinked polymers : basic principle of preparing the new class of polymeric materials. *React. Funct. Polym.*, 2002, **53** (2–3), 193–203.

(9) J.-X. Jiang, F. Su, A. Trewin, C. D. Wood and A. I. Cooper, Conjugated microporous poly(aryleneethynylene) networks. *Angew. Chem., Int. Ed.*, 2007, **46** (45), 8574–8578.

(10) A. P. Katsoulidis and M. G. Kanatzidis, Phloroglucinol based microporous polymeric organic frameworks with –OH functional groups and high CO_2 capture capacity. *Chem. Mater.*, 2011, **23** (7), 1818–1824.

(11) P. M. Budd, B. S. Ghanem, S. Makhseed, N. B. Mckeown, K. J. Msayib and C. E. Tattershall, Polymers of intrinsic microporosity (PIMs): robust, solution-processable, organic nanoporous materials. *Chem. Commun.*, 2004, (2), 230–231.

(12) N. B. Mckeown, S. Makhseed and P. M. Budd, Phthalocyanine-based nanoporous network polymers. *Chem. Commun.*, 2002, (23), 2780–2781.

(13) N. B. Mckeown, P. M. Budd and D. Book, Microporous polymers as potential hydrogen storge materials. *Macromol. Rapid Commun.*, 2007, **28** (9), 995–1002.

(14) Q. Chen, J.-X. Wang, Q. Wang, N. Bian, Z.-H. Li, C.-G. Yan and B.-H. Han, Spiro(fluorine-9,9′-xanthene)-based porous organic polymers: preparation, porosity, and exceptional hydrogen uptake at low pressure. *Macromolecules*, 2011, **44** (20), 7987–7993.

(15) B. S. Ghanem, N. B. Mckeown, P. M. Budd and D. Fritsch, Polymers of intrinsic microporosity derived from bis(phenazyl) monomers. *Macromolecules*, 2008, **41** (5), 1640–1646.

(16) B. S. Ghanem, N. B. Mckeown, P. M. Budd, J. D. Selbie and D. Fritsch,

High-performance membranes from polyimides with intrinsic microporosity. *Adv. Mater.*, 2008, **20** (14), 2766–2771.

(17) J. Weber, M. Antonietti and A. Thomas, Mesoporous poly(benzimidazole) networks *via* solvent mediated templating of hard spheres. *Macromolecules*, 2007, **40** (4), 1299–1304.

(18) M. G. Rabbani and H. M. El-Kaderi, Template-free synthesis of highly porous benzimidazole-linked polymer for CO_2 capture and H_2 storage. *Chem. Mater.*, 2011, **23** (7), 1650–1653.

(19) E. A. Steck and A. R. Day, Reactions of phenanthraquinone and retenequinone with aldehydes and ammonium acetate in acetic acid solution. *J. Am. Chem. Soc.*, 1943, **65** (3), 452–456.

(20) S. Yuan, S. Kirklin, B. Dorney, D.-J. Liu and L. Yu, Nanoporous polymers containing stereocontorted cores for hydrogen storage. *Macromolecules*, 2009, **42** (5), 1554–1559.

(21) S. S. Elmorsy, A. Pelter and K. Smith, The direct production of tri- and hexa-Substituted benzenes from ketones under mild conditions. *Tetrahedron Lett.*, 1991, **32** (33), 4175–4176.

(22) Y.-C. Zhao, Q.-Y. Cheng, D. Zhou, T. Wang and B.-H. Han, Preparation and characterization of triptycene-based microporous poly(benzimidazole) networks. *J. Mater. Chem.*, 2012, **22** (23), 11509–11514.

(23) F. Ng, D, J. Jones, J. Rozière, B. Bauer, M. Schuster and M. Jeske, Novel sulfonated poly(arylene ether benzimidazole) cardo proton conducting membranes for PEMFC. *J. Membr. Sci.*, 2010, **362** (1–2), 184–191.

(24) Y. Luo, S. Zhang, Y. Ma, W. Wang and B. Tan, Microporous organic polymers synthesized by self-condensation of aromatic hydroxymethyl monomers. *Polym. Chem.*, 2013, **4** (4), 1126–1131.

(25) B. S. Ghanem, K. J. Msayib, N. B. McKeown, K. D. M. Harris, Z. Pan, P. M. Budd, A. Butler, J. Selbie, D. Book and A. Walton, A triptycene-based polymer of intrinsic microposity that displays enhanced surfaced area and hydrogen adsorption. *Chem. Commun.*, 2007, (1), 67–69.

(26) S. S. Han, J. L. Mendoza-Cortés and W. A. Goddard, Recent advances on simulation and theory of hydrogen storage in metal–organic frameworks and covalent organic frameworks. *Chem. Soc. Rev.*, 2009, **38** (5), 1460–1476.

(27) J. Germain, J. M. J. Fréchet and F. Svec, Nanoporous polymers for hydrogen storage. *Small*, 2009, **5** (10), 1098–1111.